

PAPER

View Article Online
View Journal | View Issue



Cite this: *Environ. Sci.: Nano*, 2024, 11, 3192

The endocrine disruptor effect of metal nanoparticles mainly depends on their capacity to release metal ions†

Peggy Charbonnier,^a Pierre-Henri Jouneau^b and Aurélien Deniaud ^{*,a}

Throughout their lives, humans are constantly exposed to various pollutants that can affect our development and physiology. The growing list of pollutants include drugs, pesticides, cosmetics, plasticizers, and other organic molecules that have been found to disrupt endocrine activities. Endocrine disruptors can negatively impact our organism's development, metabolism, and sexual functions. Recently, it was discovered that exposure to silver nanoparticles (AgNP) inhibits specific liver nuclear receptors. Nuclear receptors are transcription factors that play a critical role in regulating important physiological functions including endocrine ones. To investigate further, we tested the impact of two types of metal nanoparticles: AgNP, which release metal ions, and titanium dioxide nanoparticles, which do not dissociate into ions. We found that AgNP significantly inhibited the thyroid and androgen pathways but had no effect on the aryl hydrocarbon pathway. On the other hand, titanium dioxide nanoparticles had little effect. Additionally, we observed that combining AgNP with antagonists led to cumulative inhibition of the thyroid and androgen pathways. Our previous data suggest that Ag(I) ions released from the NP trigger the inhibition of zinc finger-containing nuclear receptors. In conclusion, metal nanoparticles with a capacity to release metal ions are highly effective endocrine disruptors, and the impact caused by organic molecules co-transported with metal nanoparticles is minor.

Received 24th January 2024,
Accepted 4th June 2024

DOI: 10.1039/d4en00065j

rsc.li/es-nano

Environmental significance

Metal nanoparticles (NPs) are widely used in consumer products, which results in increased exposure to metal NPs and their by-products, leading to toxicological and ecotoxicological issues. The exposure to organic pollutants is also a growing concern. Hence, it is necessary to study multiple exposures to assess the combined impact on human health and ecosystems. In this study, exposure to silver NPs, alone or combined with organic compounds known to have an impact on endocrine functions, revealed inhibition on several pathways, while exposure to titanium dioxide NPs had minor effects. The former effect is likely due to the release of Ag(I) ions and is therefore possibly applicable to other metal NPs that can release metal ions.

Introduction

Human physiology and development are complex and finely controlled by various mechanisms, with endocrine functions playing a central role. It has become evident over the years that exposure to pollutants can affect physiology, and specific attention is focused on endocrine disruptors (ED) responsible for serious developmental issues.¹ Endocrine disruptors are generally organic molecules belonging to different chemical classes, such as pharmaceuticals, pesticides, and plasticizers (for reviews ref. 2–4). They can act as agonists or antagonists

on one or several endocrine pathways.^{5,6} Organisms are exposed to several ED or mixtures of ED, usually at low doses and throughout their lives, making it difficult to precisely quantify exposures.^{7,8} Therefore, current studies aim to describe as best as possible the impact of lifelong exposure to various mixtures of pollutants with opposing or synergistic ED effects.⁸ Another concern is the use of nanomaterials in consumer products for their valuable physico-chemical properties. However, the widespread use of nanomaterials, in particular metallic ones, results in environmental contamination and safety concerns among scientists and the general population.^{9,10} Thus, it is crucial to model the health consequences of exposure to a combination of compounds, including nanomaterials. This is challenging because the effect of mixtures is not merely the sum of the toxicity of each compound individually.

^a Univ. Grenoble Alpes, CNRS, CEA, IRIG – Laboratoire de Chimie et Biologie des Métaux, F-38000 Grenoble, France. E-mail: aurelien.deniaud@cea.fr

^b Univ. Grenoble Alpes, CEA, IRIG, MEM, F-38000 Grenoble, France

† Electronic supplementary information (ESI) available. See DOI: <https://doi.org/10.1039/d4en00065j>



There are two categories of metal nanoparticles (NP) (for review ref. 10) – persistent NP that remain in particle forms in biological conditions such as in the human body, and labile metal NP that dissolve into ions in aqueous aerobic conditions. Persistent NP includes titanium dioxide nanoparticles (TiO_2 -NP more than 10 000 tons produced per year) that are widely used in sunscreen, paints, or as food additives and can trigger particle-induced toxicity leading to inflammatory mechanisms, which could cause chronic diseases.¹¹ On the other hand, labile metal NP toxicity is primarily due to released metal ion species. Silver NP (AgNP – between 200 and 500 tons produced in 2020)¹² belongs to this category of NP. AgNP are used as biocides in various products including textiles, food packaging or medical devices, a property that requires Ag(I) ion release. However, these species are also toxic for mammals. Due to their reactivity, AgNP are dispersed in various forms in the environment. Their impact on human health and the environment has been studied for several years.^{13–17} The different forms of Ag but also TiO_2 -NPs can cross biological barriers and accumulate mainly in the liver and the kidney.^{18–20} Following endocytosis, AgNP dissolve into toxic Ag(I) ions that distributes throughout hepatocytes,²¹ and similar fate has been described in several other cell types.^{22–25}

Various studies have suggested that NP may have an impact on endocrine functions. However, most of these publications have merely described general toxicity effects on reproductive cells,^{26–28} which could be observed for any molecules and cannot be considered as a specific endocrine disruption effect. A few studies have proposed a direct impact on endocrine pathways, such as in the case of AgNP²⁹ or Cd-containing quantum dots.³⁰ This could be a result of the release of metal ions, as previously suggested in the review ref. 31.

In order to be closer to the real exposure conditions of living organisms, it is crucial to investigate the effect of co-exposure to NP and organic pollutants, particularly ED. Up to now, most of the studies indicates that NP act as carriers of organic ED, thereby increasing their potency (ref. 32 and 33 and for review ref. 34). However, some studies have found that the bioavailability of organic ED decreases when co-exposed with NP.³⁴ Therefore, comprehensive studies are required to properly analyze the impact of co-exposure to metal NP and organic ED on endocrine pathways.

In this study, we analyzed the influence of two types of metal NPs, namely TiO_2 -NP and AgNP, on three pathways: the thyroid, the androgen, and the aryl hydrocarbon pathways. The latter is not an endocrine pathway and functions using a different type of transcription factor that does not contain a zinc finger. The effect of the NP was assayed in presence of an agonist of each pathway with or without an antagonist. We observed only minor effects with TiO_2 -NP, most probably due to organic compounds binding to the NP. However, AgNP triggered significant inhibition of both thyroid and androgen

receptor activity, likely due to released Ag(I) ions that exchange with Zn(II) in the DNA binding zinc finger domain.

Methods

Experimental design

We selected two types of metal nanoparticles: PVP-coated AgNP (referred to as AgNP) and a mixture of anatase and rutile titanium dioxide nanoparticles (referred to as TiO_2 -NP). They were chosen for their wide use in consumer products and for their different behavior in aerobic conditions. Indeed, AgNP releases Ag(I) ions, while TiO_2 -NP remains stable in aqueous solutions. We tested their potential effect on the thyroid and androgen endocrine pathways, as well as on the aryl hydrocarbon pathway. The activity of the two formers relies on a Zn-finger containing nuclear receptor, while the latter is based on a helix–loop–helix transcription factor. This enabled us to test the effect on different types of transcription factors. We conducted the tests on 2D cell cultures. Initial assays were performed in presence of an agonist to have the pathway activated and to be able to observe either an increase or a decrease of the activity. Further assays were performed in presence of the same agonist at the same dose but with the addition of a second agonist or an antagonist. For the thyroid and the androgen pathways, the first agonist is physiological, *i.e.* the hormone or a derivative, T3 for the former and 17-methyltestosterone (17-MT) for the latter. For the aryl hydrocarbon pathway, we used the 2,3,7,8-tetrachlorodibenzodioxin (TCDD) that is a well-known ligand of the aryl hydrocarbon receptor.³⁵ The other agonists and antagonists used were not selected for their environmental relevance since many organic ED have multiple targets. Therefore, we choose molecules relatively selective for a pathway to precisely study the effects of NP in the different experimental set-ups. For each molecule used, a dose–response was performed to select an appropriate concentration to be used. All molecules, their effect and the chosen concentrations are summarized in the Table 1. All compounds and NPs were added simultaneously to the medium and since the cell culture assays provide a fast response, the fluorescence or luminescence data were acquired 24 hours after addition. Overall, the experiments were designed to be able to detect any kind of effects (agonist, antagonist, additive, synergistic) for both types of NP without any *a priori*. Besides, the concentrations chosen for the compounds were selected to induce agonist or antagonist effects and the NP concentrations were wide. The overall goal being to obtain mechanistic information in a first instance but the concentrations may be higher than environmentally.

Nanoparticle and mixture characterization

Econix 50 nm PVP-coated AgNP were purchased from NanoComposix and TiO_2 -NP were purchased from Sigma-Aldrich (reference 700347, mixture of anatase and rutile of less than 150 nm diameter). Before any experiment, NP stock



Table 1 List of the compounds used in this study

Molecule	Dose used	Effect
T3 hormone	100 nM	Agonist of the thyroid pathway
Amiodarone	15 μ M	Antagonist of the thyroid pathway
17-Methyltestosterone	0.1 nM	Agonist of the androgen pathway
Anastrozole	1 mg mL ⁻¹	Agonist of the androgen pathway
Linuron	5 μ M	Antagonist of the androgen pathway
2,3,7,8-Tetrachlorodibenzodioxin	10 pM	Agonist of the aryl hydrocarbon pathway
Luteolin	1 μ M	Antagonist of the aryl hydrocarbon pathway

solutions were thoroughly vortexed before dilution and addition to the proper buffer or cell culture media depending on the experiment to be performed. For cell culture experiments, the NP were not mixed with the organic compounds before addition to the cell culture. When a compound is dissolved in DMSO, it is diluted hundred times for *in vitro* or *in cellulo* experiments and a negative control at 1% DMSO is performed.

For NP characterization, UV-visible spectra were acquired on a Shimadzu UV-1800 spectrophotometer. Dynamic light scattering (DLS) measurements were carried out in water and cell culture medium corresponding to the different exposure conditions at 25 °C in a UVette (Eppendorf) on a Nanostar instrument (Wyatt). Zeta potential measurements were performed in a Litesizer 500 instrument (Anton Paar) using omega cuvette and in PBS diluted 1000 times to provide charges. The analyses were performed in the Kaliopie software. For scanning transmission electron microscopy (STEM), 5 μ L of diluted AgNP or TiO₂-NP were deposited on a glow-discharged copper grid coated with a carbon film (Mesh 300, Agar Scientific/S160N3) to limit particle agglomeration and enable even dispersion of the NP on the grid. The drop was then dried under air. STEM micrographs were taken on a Zeiss MERLIN microscope operated at 15 or 30 kV, using the solid-state bright-field detector.

Cell culture

HEK293T cells were grown in DMEM high glucose media supplemented with 10% fetal bovine serum (FBS) and 1% non-essential amino-acids at 37 °C in a humidified incubator and with an atmosphere of 5% CO₂. AR-EcoScreen and DR-EcoScreen cell lines were provided by the JCRB cell line bank (Tebu bio). AR-EcoScreen were grown in DMEM-F12 media (Gibco) supplemented with 5% FBS, 25 μ g mL⁻¹ hygromycin and 50 μ g mL⁻¹ zeocine. DR-EcoScreen were grown in MEM α media (Gibco) supplemented with 5% FBS, 1% L-Glu and 150 μ g mL⁻¹ hygromycin. All cell lines were split every 2 to 3 days to remain at a maximal confluency of 80–90%. For cell viability assays, 3.10⁵ cells were seeded in each well of a 12-well plate. On the following day, NP or AgNO₃ were added in a wide concentration range. After 24 hours of exposure, cells were rinsed with PBS, harvested using trypsin and suspended in 200 μ L PBS. Cell viability was determined by counting

trypan blue stained cells in a TC20 Automated Cell Counter (Bio-Rad).

Thyroid pathway assay

HEK293T cells were transfected with an equal amount of pCDM8-TR α (kindly provided by Professor Larsen and Assistant Professor Zavacki) and 2xDR4 developed in ref. 36 and provided by C. Cepko *via* AddGene and using a double amount of PEI, for detailed protocol see ref. 37. The next day, cells were recovered, plated in 6-well plates and exposed to the different chemicals and NP. After 24 hours of exposure, cells were recovered and GFP level was analyzed by FACS on a FACSCalibur (Becton Dickinson). Cells only exposed to 100 nM of the T3 hormone were the positive control. Indeed, T3 binds to the thyroid receptor α expressed from the pCDM8-TR α . This binding activates the thyroid receptor that subsequently binds to the DR4 DNA motif triggering the transcription of the GFP gene, finally leading to GFP protein expression and thereof fluorescence signal. The fluorescence signal in this condition was set to 100% and all other signals were normalized based on this T3 positive control condition.

Androgen and aryl hydrocarbon pathway assay

Assays of the androgen and aryl hydrocarbon pathways were performed using the AR-EcoScreen and DR-EcoScreen cell lines, respectively. These cell lines were developed and provided by Dr. Mitsuru Iida.^{38,39} The principle is to control luciferase expression by the corresponding receptors, the androgen receptor (AR) and the aryl hydrocarbon receptor (AhR) respectively, and follow their activity using the steady glow luciferase assay kit (Promega). On the first day, 20.10³ cells were seeded in black 96-well plates with transparent bottoms. On the second day, the media was changed to a media without antibiotics and with the different compounds and NP to be tested. On the third day, the luminescence signal was measured on a BioTek Synergy H1 microplate reader using the steady glow luciferase kit (Promega).

Statistical analysis

All the quantitative data presented with a standard deviation are based on at least three biological replicates. The normality was evaluated using a Shapiro–Wilk test. Statistical comparisons are based on one-way ANOVA tests with a Tukey *post hoc* tests.



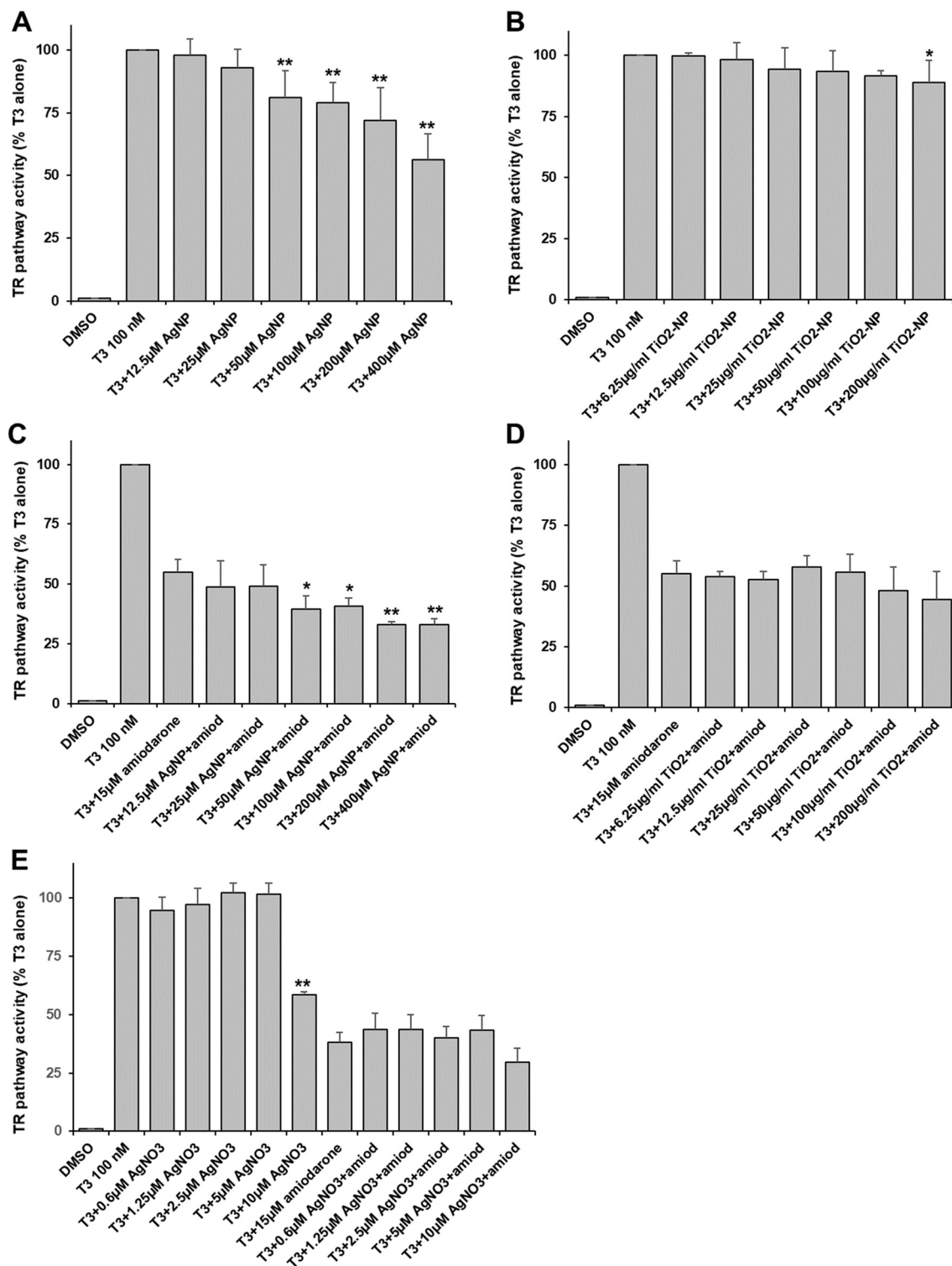


Fig. 1 Thyroid pathway activity. HEK293T cells co-transfected with the TR α receptor and GFP under the control of the thyroid receptor element (plasmid 2xDR4) were exposed to AgNP (A and C), TiO₂-NP (B and D) or AgNO₃ (E). The thyroid receptor was activated using 100 nM of the T3 hormone leading to a GFP level defined as the 100% activity. In C, D and E, co-exposure to 15 μ M of the antagonist amiodarone was done. Values represent the means \pm SD of at least three independent experiments. * stands for data statistically different from the corresponding control (T3 or T3 + amiodarone) with $p < 0.05$ and ** stands for data statistically different from the corresponding control with $p < 0.01$.



Results

Nanoparticles and mixture characterization

We characterized in depth AgNP and TiO₂-NP used in this study. STEM analysis showed well-dispersed AgNP with a main population of 30 to 80 nm diameter and a second population of smaller particles (Fig. S1A†). As expected, TiO₂-NP are heavily agglomerated and the primary particles have a diameter smaller than 50 nm (Fig. S1B†). UV-visible spectra showed absorbance in the UV range for both types of NP and a specific peak with a maximum around 400 nm for AgNP that is due to the plasmon resonance (Fig. S1C†). The hydrodynamic status of both AgNP and TiO₂-NP was analysed by DLS, in water and in the different relevant cell culture media, alone or in the presence of different compounds used for cell culture experiments. In parallel, the zeta potential of the different mixtures was determined in diluted PBS. All the data are presented in the Table S1.† In water, AgNP were homogenous (polydispersity index (PDI) of 6.3%) with an average hydrodynamic diameter of 52.6 nm and a zeta potential of −16.3 mV. In the different complete cell culture media, AgNP had a larger diameter between 60 and 70 nm, most probably due to the formation of a surrounding protein corona. Diameter distribution was also wider with a polydispersity between 10 and 25%. Most of the compounds did not significantly impact AgNP dispersion. However, 17-MT improved AgNP diameter dispersion in water and cell culture media, while amiodarone increased diameter in water and improved homogeneity in cell culture media. Interestingly, 17-MT, amiodarone but also anastrozole induced an increase of the zeta potential to about −3/−4 mV. These data led us to hypothesize that these compounds can associate with AgNP.

The TiO₂-NP we used had a primary particle of 20 nm in diameter. In water, we obtained a homogenous hydrodynamic diameter of 200 nm (PDI of 11.4%), which probably indicates the formation of clusters of a few particles together. In addition, TiO₂-NP had a zeta potential of −38.3 mV. In complete cell culture media, TiO₂-NP formed polydisperse and large agglomerates ranging from 400 nm to a few micrometers in diameter, regardless of the presence of serum protein or the addition of different compounds. In water, the T3 hormone and amiodarone increased agglomerate diameter slightly and more than doubled the PDI. Amiodarone also importantly increased zeta potential to −6.8 mV. This suggests that T3 and amiodarone may bind to TiO₂-NP.

Thyroid pathway

In order to evaluate the effects of AgNP and TiO₂-NP on the thyroid pathway, we established a reporter system in HEK293T cells. This system ensured that the expression of GFP was regulated by the TR α which was activated by the T3 hormone. Viability assays showed that the viability of HEK293T cells started decreasing when they were exposed to 400 μ M of AgNP or 200 μ g ml^{−1} of TiO₂-NP (Table S2†), which

were the highest concentrations used for the assessment of the thyroid pathway.

On the one hand, TR activity was dose-dependently inhibited upon the addition of AgNP at concentrations higher than 50 μ M in Ag (Fig. 1A). The inhibition reached up to 50% at 400 μ M. On the other hand, TiO₂-NP only led to minor and mainly insignificant inhibition (10–15%) at concentrations in particle higher than 25 μ g ml^{−1} (Fig. 1B). In a second set-up, we used amiodarone, a known endocrine disruptor with antagonist activity on this pathway⁴⁰ at a concentration that inhibited about half of the activity triggered by T3. Under these conditions, AgNP had an additive inhibitory effect at concentrations higher than 50 μ M, leading to about 70% inhibition of the thyroid receptor activity (Fig. 1C). Therefore, amiodarone and AgNP have a cumulative but not synergistic impact on the thyroid receptor pathway. In the case of TiO₂-NP, there was no significant cumulative inhibition observed due to these NP (Fig. 1D).

Since it is known that AgNP can release Ag(i) ions in the media and inside cells, we assessed the impact of an Ag salt (AgNO₃) on the thyroid pathway. We used concentrations up to 10 μ M to avoid the toxicity of the Ag(i) ions. We observed a very specific behavior with AgNO₃. No effect was observed at concentrations up to 5 μ M but 10 μ M led to an important inhibition of more than 40% (Fig. 1E), suggesting that a threshold was reached. In the presence of amiodarone, no significant additive inhibition was observed with AgNO₃, but an inhibition was observed at 10 μ M of AgNO₃ (Fig. 1E).

Androgen pathway

We found that AgNP and TiO₂-NP caused significant toxicity in AR-EcoScreen cells at concentrations of 200 μ M and 50 μ g ml^{−1}, respectively (Table S2†). The AR pathway was activated by the addition of 17-MT. Our results showed that AgNP significantly inhibited the androgen receptor activity in a dose-dependent manner starting at 12.5 μ M in Ag, and leading to 60% inhibition at 100 μ M (Fig. 2A). However, exposure to TiO₂-NP did not produce any inhibitory effect on the androgen pathway (Fig. 2B). To investigate the impact of mixtures with ED, we tested the effects of anastrozole and linuron, which are an agonist and an antagonist, respectively, of the androgen pathway. We found that in the presence of anastrozole and AgNP the androgen pathway was drastically inhibited, leading to 50% inhibition at the lowest concentration of AgNP and up to 65% inhibition at 100 μ M Ag (Fig. 2C). However, there is an important variability for part of these data and the AgNP-induced inhibition in the presence of an agonist is drastic and not trivial to explain. When tested in the presence of linuron, the combination of linuron and AgNP resulted in additive inhibition, leading to 80% inhibition of the androgen receptor activity with linuron plus 100 μ M AgNP (Fig. 2C). Co-exposure with TiO₂-NP resulted in a significant inhibition of the activation induced by anastrozole at concentrations of 6.25 and 100 μ g ml^{−1}





Fig. 2 Androgen pathway activity. AR-EcoScreen cells were exposed to AgNP (A and C) or TiO₂-NP (B and D). The androgen receptor was activated using 0.1 nM 17-MT leading to a luciferase level defined as the 100% activity. In C and D, co-exposure to either 1 mg ml⁻¹ of the agonist anastrozole or to 5 μM of the antagonist linuron was done. Values represent the means ± SD of at least three independent experiments. * stands for data statistically different from the corresponding control (17-MT or 17-MT + anastrozole or 17-MT + linuron) with $p < 0.05$ and ** stands for data statistically different from the corresponding control with $p < 0.01$.

(Fig. 2D), while the effect of linuron was not significantly modified by TiO₂-NP (Fig. 2D).

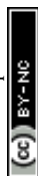
Aryl hydrocarbon pathway

We found that TiO₂-NP caused significant toxicity in DR-EcoScreen cells at concentrations of 50 μg ml⁻¹ (Table S2†), while AgNP was not toxic at all up to 400 μM. The activation of the AhR pathway was induced by TCDD, and the effect of AgNP and TiO₂-NP on the pathway was studied. The activation of the aryl hydrocarbon pathway was not significantly affected by AgNP (Fig. 3A) and TiO₂-NP led to a low but non-significant inhibition of AhR activity at concentrations between 25 and 100 μg ml⁻¹ (Fig. 3B). Furthermore, the experiments were conducted with luteolin as an antagonist of AhR. The addition of increasing concentrations of AgNP or TiO₂-NP did not cause any significant effect compared to the mixture of agonist and antagonist of the AhR alone (Fig. 3C and D). The findings

showed that AgNP and TiO₂-NP have no significant effect on the aryl hydrocarbon pathway.

Discussion

In this study, we evaluated the impact of two types of metal nanoparticles – AgNP and TiO₂-NP – on three ligand-activated transcription pathways in mammalian cells. Our goal was to determine whether these nanoparticles could potentially disrupt endocrine functions. TiO₂-NP is a stable particle that remains intact in cell culture media and after being taken up by mammalian cells. In contrast, AgNP releases Ag(I) ions in aerobic conditions, which means that mammalian cells are exposed to both the nanoparticles and the associated ions. When exposed to hormones or organic compounds that have known effects on the activity of the transcription pathways, the nanoparticles could affect their bioavailability by either facilitating their transport into the cells or trapping them outside the cells. This could have a positive or negative



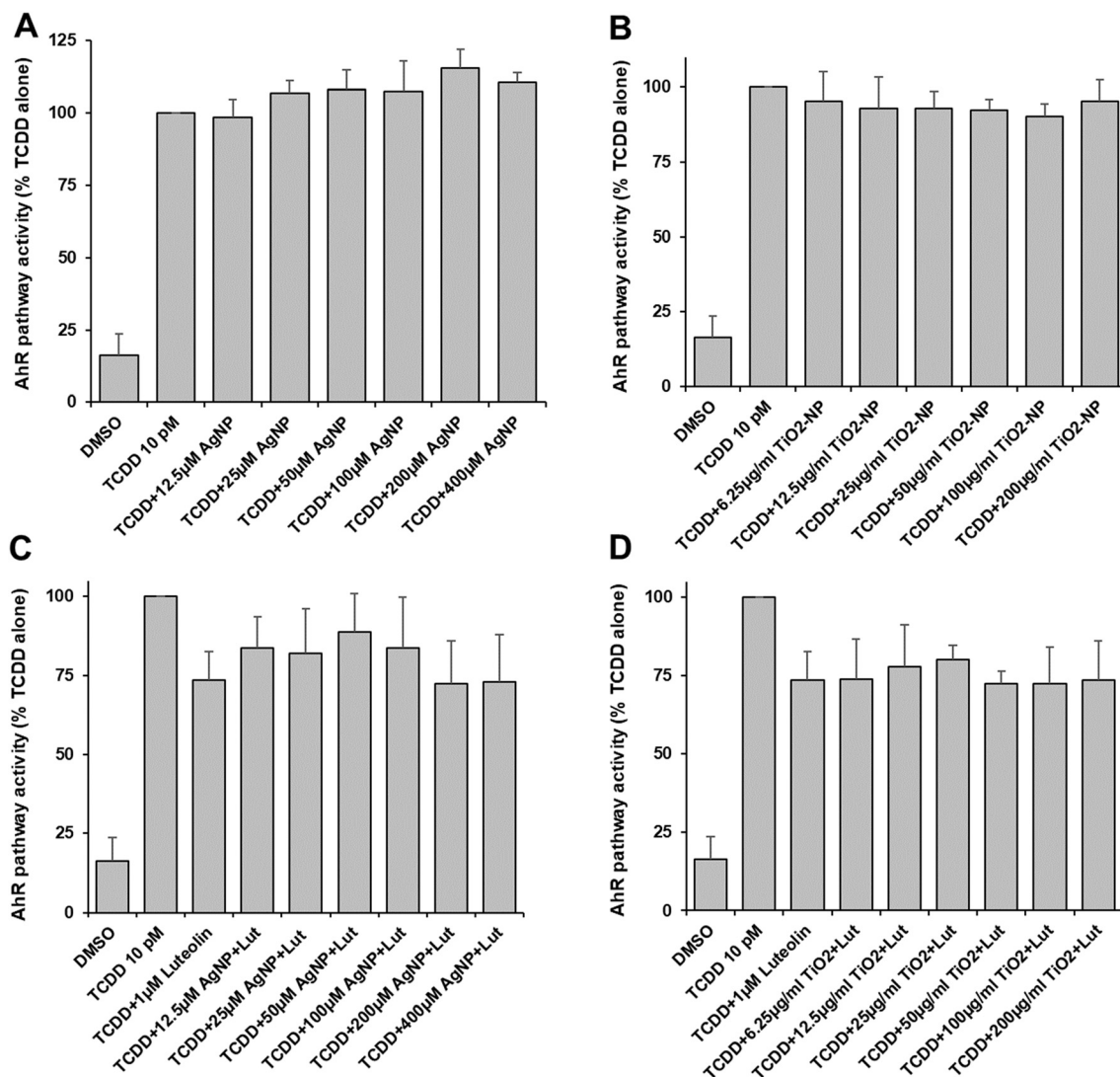


Fig. 3 Aryl hydrocarbon pathway activity. DR-EcoScreen cells were exposed to AgNP (A and C) or TiO₂-NP (B and D). The aryl hydrocarbon receptor was activated using 10 pM TCDD leading to a luciferase level defined as the 100% activity. In C and D, co-exposure to 1 μM of the antagonist luteolin was done. Values represent the means ± SD of at least three independent experiments.

impact on the selected pathway. To distinguish between these different effects, we conducted a thorough investigation that involved *in vitro* analysis using DLS and biological effect assessment through reporter gene systems. We tested two nuclear receptor-dependent pathways (thyroid and androgen) and the aryl hydrocarbon pathway, which is not related to a nuclear receptor.

In the three examined pathways, TiO₂-NP caused only minor effects, which were limited to a 20% inhibition of the tested receptor activity. These effects were observed only at high concentrations of particles, at least 25 μg ml⁻¹. This was observed in the thyroid pathway and the androgen pathway when co-exposed with 17-MT and anastrozole. Interestingly, most of the organic compounds tended to increase the polydispersity or even led to the formation of larger aggregates of TiO₂-NP (Table S1†). Therefore, the observed cellular effects at high concentrations in TiO₂-NP are most

likely due to an interaction between the organic compounds and the NP, which inhibits the agonistic activity and has a neutral effect when co-exposed with an agonist and an antagonist.

It was observed that AgNP did not affect the AhR pathway, while dose-dependent inhibition was observed for the two nuclear receptor pathways that were assessed. When exposed to agonists, AgNP led to more than 50% inhibition, and a cumulative effect was observed when co-exposed with antagonists. Strong inhibition was similarly observed upon exposure to few micromolars of a silver salt providing a direct source of Ag(I) ions. Therefore, it can be concluded that the AgNP-induced inhibition of nuclear receptor pathways is mainly, if not completely, due to the released Ag(I) ions. The main difference between the nuclear receptors and the aryl hydrocarbon receptor is the motif they contain to bind their DNA cognate motif. A zinc finger domain is present in the



former, while a helix-loop-helix domain is present in the latter. Previously, we have shown that hepatocyte exposure to AgNP led to the inhibition of the farnesyl X-receptor (FXR) and even more pronounced of the liver X-receptor (LXR) in hepatocytes.¹⁶ Elemental imaging enabled us to show that AgNP exposure in hepatocytes leads to the release of Ag(I) ions and their partial translocation to the nucleus. We hypothesized that the inhibition of FXR and LXR could be attributed to the exchange of Zn(II) by Ag(I) in their zinc finger DNA binding domain, which comprises the tetra-cysteine domain. Ag(I) has a higher affinity for this amino-acid than Zn(II). Our hypothesis was confirmed *in vitro* on model zinc finger peptides with two, three, and four cysteines. These peptides showed at least three orders of magnitude higher affinity for Ag(I) compared to Zn(II).⁴¹ Ag(I) forms multinuclear clusters (Ag_xS_x motifs) in these domains, leading to the loss of the finger structure and hence, the inability to bind to its cognate DNA motifs.^{41,42} Additionally, a model protein in the presence of DNA also revealed that Ag(I) can compete with Zn(II) in a zinc finger domain already bound to its cognate DNA.⁴² The data collected indicates that Ag(I) ions released from AgNP can compete with Zn(II) in zinc finger domain, even in already assembled and highly structured complexes, thereby preventing the interaction of zinc finger domains with their partners and thus impacting their associated activity. The present study showed that this effect can be generalized to the inhibition of critical nuclear receptors which are involved in endocrine functions such as the thyroid and androgen receptors. This means that exposure to AgNP can induce an endocrine disruptor activity that can be cumulative with the effect of antagonists. The endocrine disruptor effect of metal NP is mainly due to the released metal ions. Therefore, future design of metal-based nanomaterials should favor the development of structures that protect the nanomaterial from releasing metal ions. It is important to note that the effect observed with AgNP could extend to other types of metal-NP that release metal ions in biological conditions such as CuO-NP or CdNP such as in Cd quantum dots that have already shown endocrine disruptor effects.³⁰ The intensity of the endocrine disruption would depend on the amount of released ions in cells and the ratio between the affinity of the released ions and the physiological Zn(II) ions, which is highly favorable in the case of AgNP.

Conclusions

In summary, this study reported the inhibitory effect of AgNP on nuclear receptor-dependent endocrine pathways such as the thyroid or the androgen pathways. This effect is due to a direct action of Ag(I) ions released from the NP. On the other hand, TiO₂-NP only showed mild effect that are due to their interaction with the organic compounds tested that can either decrease or increase their cellular uptake depending on the cases. These tendencies can most probably be extended to other metal releasing nanoparticles and to rock

solid metal nanoparticles for the cases of AgNP and TiO₂-NP, respectively. Finally, although these experiments have been performed on mammalian cells, similar endocrine disruptions can occur in various organisms with nuclear receptors. Our findings are thus opening a door concerning the analysis of the impact of metal NP on endocrine disruptions as well as of mixture between metal NP and organic pollutants.

Author contributions

AD conceived the project and designed the study. PC, PHJ and AD performed the experiments. PC and AD participated in data analysis. AD wrote the manuscript.

Conflicts of interest

Authors have no competing interests to declare.

Acknowledgements

This project received funding from GRAL, the Grenoble Alliance for Integrated Structural & Cell Biology, a program from the Chemistry Biology Health Graduate School of University Grenoble Alpes (ANR-17-EURE-0003). This project was supported by the French National Research Program for Environmental and Occupational Health of Anses (2019/1/184). We acknowledge Professor Larsen and Assistant Professor Zavacki for providing pCDM8-TR plasmids and Dr Mitsuru Iida that provided the AR-EcoScreen and DR-EcoScreen cell lines. We thank the staff of the BIOMade platform for their technical assistance with the zeta potential measurements.

References

- 1 E. R. Kabir, M. S. Rahman and I. Rahman, A review on endocrine disruptors and their possible impacts on human health, *Environ. Toxicol. Pharmacol.*, 2015, **40**, 241–258.
- 2 T. Kek, K. Geršak and I. Virant-Klun, Exposure to endocrine disrupting chemicals (bisphenols, parabens, and triclosan) and their associations with preterm birth in humans, *Reprod. Toxicol.*, 2024, **125**, 108580.
- 3 T. J. Woodruff, Health Effects of Fossil Fuel-Derived Endocrine Disruptors, *N. Engl. J. Med.*, 2024, **390**, 922–933.
- 4 L. Calero-Medina, M. J. Jimenez-Casquet, L. Heras-Gonzalez, J. Conde-Pipo, A. Lopez-Moro, F. Olea-Serrano and M. Mariscal-Arcas, Dietary exposure to endocrine disruptors in gut microbiota: A systematic review, *Sci. Total Environ.*, 2023, **886**, 163991.
- 5 Z. Dang, Amphibian toxicity testing for identification of thyroid disrupting chemicals, *Environ. Pollut.*, 2022, **311**, 120006.
- 6 M. Jeřeta, J. Navrátilová, K. Franzová, S. Fialková, B. Kempisty, P. Ventruba, J. Žáková and I. Crha, Overview of the Mechanisms of Action of Selected Bisphenols and



- Perfluoroalkyl Chemicals on the Male Reproductive Axes, *Front. Genet.*, 2021, **12**, 692897.
- 7 N. Papaioannou, E. Distel, E. de Oliveira, C. Gabriel, I. S. Frydas, O. Anesti, E. A. Attignon, A. Odena, R. Díaz, M. Aggerbeck, M. Horvat, R. Barouki, S. Karakitsios and D. A. Sarigiannis, Multi-omics analysis reveals that co-exposure to phthalates and metals disturbs urea cycle and choline metabolism, *Environ. Res.*, 2021, **192**, 110041.
 - 8 T. Tralau, M. Oelgeschläger, J. Kugler, D. Bloch, A. Braeuning, T. Burgdorf, P. Marx-Stoelting, V. Ritz, S. Schmeisser, A. Trubiroha, S. Zellmer, A. Luch, G. Schönfelder, R. Solecki and A. Hensel, A prospective whole-mixture approach to assess risk of the food and chemical exposome, *Nat. Food*, 2021, **2**, 463–468.
 - 9 C. Miao, P. Jia, C. Luo, J. Pang, L. Xiao, T. Zhang, J. Duan, Y. Li and Z. Sun, The size-dependent in vivo toxicity of amorphous silica nanoparticles: A systematic review, *Ecotoxicol. Environ. Saf.*, 2024, **271**, 115910.
 - 10 M. Chevallet, G. Veronesi, A. Fuchs, E. Mintz, I. Michaud-Soret and A. Deniaud, Impact of labile metal nanoparticles on cellular homeostasis. Current developments in imaging, synthesis and applications, *Biochim. Biophys. Acta, Gen. Subj.*, 2017, **1861**, 1566–1577.
 - 11 S. Bettini, E. Boutet-Robinet, C. Cartier, C. Coméra, E. Gaultier, J. Dupuy, N. Naud, S. Taché, P. Grysan, S. Reguer, N. Thieriet, M. Réfrégiers, D. Thiaudière, J.-P. Cravedi, M. Carrière, J.-N. Audinot, F. H. Pierre, L. Guzylack-Piriou and E. Houdeau, Food-grade TiO₂ impairs intestinal and systemic immune homeostasis, initiates preneoplastic lesions and promotes aberrant crypt development in the rat colon, *Sci. Rep.*, 2017, **7**, 40373.
 - 12 S. Temizel-Sekeryan and A. L. Hicks, Global environmental impacts of silver nanoparticle production methods supported by life cycle assessment, *Resour., Conserv. Recycl.*, 2020, **156**, 104676.
 - 13 A. E. Pradas del Real, V. Vidal, M. Carrière, H. Castillo-Michel, C. Levard, P. Chaurand and G. Sarret, Silver Nanoparticles and Wheat Roots: A Complex Interplay, *Environ. Sci. Technol.*, 2017, **51**, 5774–5782.
 - 14 T. Wang, P. Marle, V. I. Slaveykova, K. Schirmer and W. Liu, Comparative study of the sensitivity of two freshwater gastropods, *Lymnaea stagnalis* and *Planorbis* *corneus*, to silver nanoparticles: bioaccumulation and toxicity, *Environ. Pollut.*, 2022, **312**, 119999.
 - 15 J. Jia, F. Li, H. Zhou, Y. Bai, S. Liu, Y. Jiang, G. Jiang and B. Yan, Oral Exposure to Silver Nanoparticles or Silver Ions May Aggravate Fatty Liver Disease in Overweight Mice, *Environ. Sci. Technol.*, 2017, **51**, 9334–9343.
 - 16 V. Tardillo Suárez, E. Karepina, M. Chevallet, B. Gallet, C. Cottet-Rousselle, P. Charbonnier, C. Moriscot, I. Michaud-Soret, W. Bal, A. Fuchs, R. Tucoulou, P.-H. Jouneau, G. Veronesi and A. Deniaud, Nuclear translocation of silver ions and hepatocyte nuclear receptor impairment upon exposure to silver nanoparticles, *Environ. Sci.: Nano*, 2020, **7**, 1373–1387.
 - 17 Y. Rekik, V. Tardillo Suárez, V. R. Sharma, M. Chevallet, B. Gallet, D. Falconet, P. Charbonnier, I. Kieffer, R. Tucoulou, P.-H. Jouneau, G. Veronesi and A. Deniaud, Deciphering silver nanoparticle fate in liver up to biliary excretion using HepG2/C3A spheroids in scenarios mimicking different exposure pathways, *Environ. Sci.: Nano*, 2023, **10**, 1842–1857.
 - 18 E. Brun, F. Barreau, G. Veronesi, B. Fayard, S. Sorieul, C. Chanéac, C. Carapito, T. Rabilloud, A. Mabondzo, N. Herlin-Boime and M. Carrière, Titanium dioxide nanoparticle impact and translocation through ex vivo, in vivo and in vitro gut epithelia, *Part. Fibre Toxicol.*, 2014, **11**, 13.
 - 19 K. Loeschner, N. Hadrup, K. Qvortrup, A. Larsen, X. Gao, U. Vogel, A. Mortensen, H. R. Lam and E. H. Larsen, Distribution of silver in rats following 28 days of repeated oral exposure to silver nanoparticles or silver acetate, *Part. Fibre Toxicol.*, 2011, **8**, 18.
 - 20 M. van der Zande, R. J. Vandebriel, E. Van Doren, E. Kramer, Z. Herrera Rivera, C. S. Serrano-Rojero, E. R. Gremmer, J. Mast, R. J. B. Peters, P. C. H. Hollman, P. J. M. Hendriksen, H. J. P. Marvin, A. A. C. M. Peijnenburg and H. Bouwmeester, Distribution, Elimination, and Toxicity of Silver Nanoparticles and Silver Ions in Rats after 28-Day Oral Exposure, *ACS Nano*, 2012, **6**, 7427–7442.
 - 21 G. Veronesi, A. Deniaud, T. Gallon, P.-H. Jouneau, J. Villanova, P. Delangle, M. Carrière, I. Kieffer, P. Charbonnier, E. Mintz and I. Michaud-Soret, Visualization, quantification and coordination of Ag⁺ ions released from silver nanoparticles in hepatocytes, *Nanoscale*, 2016, **8**, 17012–17021.
 - 22 V. De Matteis, M. A. Malvindi, A. Galeone, V. Brunetti, E. De Luca, S. Kote, P. Kshirsagar, S. Sabella, G. Bardi and P. P. Pompa, Negligible particle-specific toxicity mechanism of silver nanoparticles: the role of Ag⁺ ion release in the cytosol, *Nanomedicine*, 2015, **11**, 731–739.
 - 23 X. Jiang, T. Miclăuş, L. Wang, R. Foldbjerg, D. S. Sutherland, H. Autrup, C. Chen and C. Beer, Fast intracellular dissolution and persistent cellular uptake of silver nanoparticles in CHO-K1 cells: implication for cytotoxicity, *Nanotoxicology*, 2015, **9**, 181–189.
 - 24 G. Veronesi, C. Aude-Garcia, I. Kieffer, T. Gallon, P. Delangle, N. Herlin-Boime, T. Rabilloud and M. Carrière, Exposure-dependent Ag⁺ release from silver nanoparticles and its complexation in AgS₂ sites in primary murine macrophages, *Nanoscale*, 2015, **7**, 7323–7330.
 - 25 L. Wang, T. Zhang, P. Li, W. Huang, J. Tang, P. Wang, J. Liu, Q. Yuan, R. Bai, B. Li, K. Zhang, Y. Zhao and C. Chen, Use of Synchrotron Radiation-Analytical Techniques To Reveal Chemical Origin of Silver-Nanoparticle Cytotoxicity, *ACS Nano*, 2015, **9**, 6532–6547.
 - 26 I. Iavicoli, L. Fontana, V. Leso and A. Bergamaschi, The Effects of Nanomaterials as Endocrine Disruptors, *Int. J. Mol. Sci.*, 2013, **14**, 16732–16801.
 - 27 T. Komatsu, M. Tabata, M. Kubo-Irie, T. Shimizu, K. Suzuki, Y. Nihei and K. Takeda, The effects of nanoparticles on mouse testis Leydig cells in vitro, *Toxicol. In Vitro*, 2008, **22**, 1825–1831.



- 28 S. Yoshida, K. Hiyoshi, T. Ichinose, H. Takano, S. Oshio, I. Sugawara, K. Takeda and T. Shibamoto, Effect of nanoparticles on the male reproductive system of mice, *Int. J. Androl.*, 2009, **32**, 337–342.
- 29 Z. Wang, Q. Li, L. Xu, J. Ma, B. Wei, Z. An, W. Wu and S. Liu, Silver nanoparticles compromise the development of mouse pubertal mammary glands through disrupting internal estrogen signaling, *Nanotoxicology*, 2020, **14**, 740–756.
- 30 M. P. Jain, F. Vaisheva and D. Maysinger, Metalloestrogenic effects of quantum dots, *Nanomedicine*, 2012, **7**, 23–37.
- 31 I. Iavicoli, L. Fontana and A. Bergamaschi, The Effects of Metals as Endocrine Disruptors, *J. Toxicol. Environ. Health, Part B*, 2009, **12**, 206–223.
- 32 Q. Fang, Q. Shi, Y. Guo, J. Hua, X. Wang and B. Zhou, Enhanced Bioconcentration of Bisphenol A in the Presence of Nano-TiO₂ Can Lead to Adverse Reproductive Outcomes in Zebrafish, *Environ. Sci. Technol.*, 2016, **50**, 1005–1013.
- 33 Y. Guo, L. Chen, J. Wu, J. Hua, L. Yang, Q. Wang, W. Zhang, J.-S. Lee and B. Zhou, Parental co-exposure to bisphenol A and nano-TiO₂ causes thyroid endocrine disruption and developmental neurotoxicity in zebrafish offspring, *Sci. Total Environ.*, 2019, **650**, 557–565.
- 34 S. Naasz, R. Altenburger and D. Kühnel, Environmental mixtures of nanomaterials and chemicals: The Trojan-horse phenomenon and its relevance for ecotoxicity, *Sci. Total Environ.*, 2018, **635**, 1170–1181.
- 35 A. Poland, E. Glover and A. S. Kende, Stereospecific, high affinity binding of 2,3,7,8-tetrachlorodibenzo-p-dioxin by hepatic cytosol. Evidence that the binding species is receptor for induction of aryl hydrocarbon hydroxylase, *J. Biol. Chem.*, 1976, **251**, 4936–4946.
- 36 N. A. Billings, M. M. Emerson and C. L. Cepko, Analysis of Thyroid Response Element Activity during Retinal Development, *PLoS One*, 2010, **5**, e13739.
- 37 A. Deniaud, M. Karuppasamy, T. Bock, S. Masiulis, K. Huard, F. Garzoni, K. Kerschgens, M. W. Hentze, A. E. Kulozik, M. Beck, G. Neu-Yilik and C. Schaffitzel, A network of SMG-8, SMG-9 and SMG-1 C-terminal insertion domain regulates UPF1 substrate recruitment and phosphorylation, *Nucleic Acids Res.*, 2015, **43**, 7600–7611.
- 38 K. Satoh, K. Ohyama, N. Aoki, M. Iida and F. Nagai, Study on anti-androgenic effects of bisphenol a diglycidyl ether (BADGE), bisphenol F diglycidyl ether (BFDGE) and their derivatives using cells stably transfected with human androgen receptor, AR-EcoScreen, *Food Chem. Toxicol.*, 2004, **42**, 983–993.
- 39 S. Takeuchi, M. Iida, H. Yabushita, T. Matsuda and H. Kojima, In vitro screening for aryl hydrocarbon receptor agonistic activity in 200 pesticides using a highly sensitive reporter cell line, DR-EcoScreen cells, and in vivo mouse liver cytochrome P450-1A induction by propanil, diuron and linuron, *Chemosphere*, 2008, **74**, 155–165.
- 40 M. F. Norman and T. N. Lavin, Antagonism of thyroid hormone action by amiodarone in rat pituitary tumor cells, *J. Clin. Invest.*, 1989, **83**, 306–313.
- 41 K. Kluska, M. D. Peris-Díaz, D. Płonka, A. Moysa, M. Dadlez, A. Deniaud, W. Bal and A. Krężel, Formation of highly stable multinuclear Ag_nS_n clusters in zinc fingers disrupts their structure and function, *Chem. Commun.*, 2020, **56**, 1329–1332.
- 42 K. Kluska, G. Veronesi, A. Deniaud, B. Hajdu, B. Gyurcsik, W. Bal and A. Krężel, Structures of Silver Fingers and a Pathway to Their Genotoxicity, *Angew. Chem., Int. Ed.*, 2022, **61**(12), e202116621.

